BIOCHEMISTRY
including biophysical chemistry & molecular biology

Article

pubs.acs.org/biochemistry

Why the *Drosophila* Shaker K^+ Channel Is Not a Good Model for Ligand Binding to Voltage-Gated Kv1 Channels

Somayeh Mahdavi and Serdar Kuyucak*

School of Physics, University of Sydney, Sydney, New South Wales 2006, Australia

Supporting Information

ABSTRACT: The *Drosophila* Shaker K^+ channel is the first cloned voltage-gated potassium channel and has, therefore, played an important role in structural and functional studies of those channels. While such a role is well justified for ion permeation, it is not clear whether this also extends to ligand binding. Despite the high degree of homology among Shaker and Kv1 channels, κ-conotoxin PVIIA (κ-PVIIA) binds to Shaker with high affinity but not to Kv1 channels. Here we address this issue by studying binding of κ-PVIIA to Shaker and Kv1 channels using molecular dynamics (MD) simulations. The structures of the channel−toxin complexes are constructed via docking and refinement with MD. The binding mode of each complex is characterized and compared to available mutagenesis data to validate the complex models. The potential of mean force for dissociation of the Shaker−κ-PVIIA complex is calculated from umbrella sampling MD simulations, and the corresponding binding free energy is determined, which provides further validation of the complex structure. Comparison of the Shaker and Kv1 complex models shows that a few mutations in the turret and extended regions are sufficient to abolish the observed sensitivity of Shaker to κ-PVIIA. This study demonstrates that Shaker is not always a good model for Kv1 channels for ligand binding. It also provides insights into the binding of the toxin to potassium channels that will be useful for improving affinity and selectivity properties of Kv1 channels.

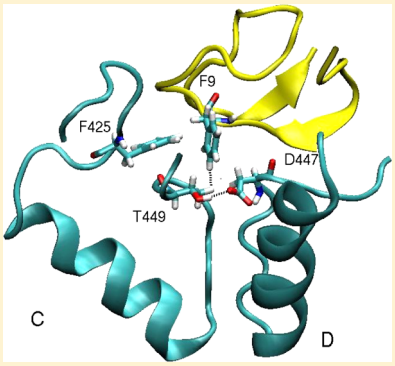

The Shaker-related family of voltage-gated potassium channels (Kv1)[1,2] regulate the membrane potential in neurons, lymphocytes, and heart, muscle, and kidney cells and thereby play an important role in the function of excitable cells.[1−3] Because of their prominent role in the nervous system, Kv1 channels have been the targets of many toxins from venomous animals, which bind and block the channels with high affinity.[4−6] In the absence of crystal structures, such toxins have been profitably used in physiological studies to probe the structure and function of ion channels.[1,2,7−9] Peptide toxins that bind to ion channels with high affinity also provide promising candidates for the development of drugs targeting ion channels.[10−12] Examples include ShK toxin from sea anemone targeting Kv1.3 for the treatment of autoimmune diseases,[13,14] μ-conotoxins and spider toxins targeting Nav1 channels for chronic pain,[15,16] and α-conotoxins targeting nicotinic acetylcholine receptor channels for pain treatment.[17,18]

The *Drosophila* Shaker (Shaker) channel is the first voltage-gated potassium channel to be cloned,[19,20] and because of this, it is often used as a role model in the investigation of structure−function relations in Kv1 channels.[1] This role is well-justified for the ion permeation problem as confirmed by numerous single-channel conductance studies[1] and can be rationalized by the fact that the sequences of the selectivity filter and pore helix are highly conserved among Shaker and Kv1 channels.[21] For the ligand binding problem, however, the experimental data from toxins are not uniformly supportive in this regard. For example, κ-conotoxin PVIIA (κ-PVIIA) binds to Shaker with high affinity but not to Kv1 channels,[22,23] while κM-conotoxin RIIIK binds to both Shaker and Kv1.2 with similar affinity.[24,25] Such variations are clearly caused by differences in the extracellular interface, which plays an important role in toxin binding. Indeed, sequence alignment in the extracellular interface region shows several differences in the functional residues of Shaker and Kv1 channels.[21] To understand why Shaker is not always a good model for the binding of ligand to Kv1 channels, one needs to relate these structural differences to the functional data for toxin binding, and this requires construction of accurate models of channel−toxin complexes.

At present, the combination of docking methods with molecular dynamics (MD) simulations provides an optimal computational method for accurate determination of protein−ligand complexes.[26] The feasibility and accuracy of this approach for toxin ligands were demonstrated on a potassium channel−charybdotoxin complex,[27,28] where the complex structure was determined by nuclear magnetic resonance (NMR).[29] In these studies, it was also shown that the binding free energy of the toxin could be calculated near chemical accuracy using umbrella sampling MD simulations. Thus, one can use the binding free energy calculations to validate a model complex structure obtained from docking and MD simulations. We note that mutagenesis experiments provide more detailed

Received: September 14, 2012
Revised: January 16, 2013
Published: February 11, 2013

 © 2013 American Chemical Society dx.doi.org/10.1021/bi301257p | *Biochemistry* 2013, 52, 1631−1640

Table 1. Alignment of the Shaker and Kv1 Channel Sequences Depicting the Differences in the Turret and Extended Regions

		turret	pore helix	filter	extended region	
Shaker	418	EA**GSENSFFK**	SIPDAFWWAVV**T**MT	TVGYG	DM**TPVGVW**	454
Kv1.1	348	EA**EEAESHFS**	SIPDAFWWAVV**S**MT	TVGYG	DM**YPVTIG**	384
Kv1.2	350	EA**DERDSQFP**	SIPDAFWWAVV**S**MT	TVGYG	DM**VPTTIG**	386

tests for a given model complex but are much harder to perform and, therefore, not as commonly available as the binding affinities.

The docking and MD simulation approach has been adapted in several recent studies of binding of toxin to ion channels.[30−34] Here we use this approach to study binding of κ-PVIIA to Shaker and two types of Kv1 channels (Kv1.1 and Kv1.2), which are most homologous to Shaker. κ-PVIIA was the first conotoxin found to block the voltage-gated potassium channel Shaker,[22] and therefore, it has attracted a great deal of attention. Its structure was determined by NMR,[35,36] and its mode of binding to Shaker was studied via mutagenesis experiments.[23,37] κ-PVIIA has also been used in many functional studies of Shaker channels.[38−41] Structure and mutagenesis data indicate that κ-PVIIA binds to Shaker via a functional dyad consisting of a pore-inserting lysine (K7) and a hydrophobic residue (F9), similar to the binding mode of other toxin blockers of potassium channels.[42,43]

Binding of κ-PVIIA to Shaker was previously studied using a combination of Brownian and molecular dynamics simulations.[44] Although the functional dyad was reproduced in the predicted complex structure, several other charge interactions identified in ref 44 were in disagreement with the mutagenesis data.[37] Here we aim to find a Shaker−κ-PVIIA complex that is consistent with the mutagenesis data. We also construct the potential of mean force (PMF) for κ-PVIIA and determine its binding free energy, as well as calculating the free energy change resulting from mutations. These free energy calculations provide further validation of the proposed Shaker−κ-PVIIA complex. Finally, we construct models for Kv1.1 and Kv1.2 in complex with κ-PVIIA and contrast their binding modes with that of Shaker. Our results provide a mechanistic understanding of why κ-PVIIA binds to Shaker with high affinity but not to Kv1.1 and Kv1.2 channels.

METHODS

Modeling of Shaker and Kv1.1 Channels. The crystal structure of the rat Kv1.2 channel is available [Protein Data Bank (PDB) entry 2R9R],[45] and we use this structure to construct homology models for rat Kv1.1 and *Drosophila* Shaker channels (rat Kv1 channels are chosen because the functional data were obtained for these channels). The sequences of the three channels are taken from the UniProt database (Shaker, P08510; Kv1.1, P10449; Kv1.2, P63142). Because the voltage sensor domain (S1−S4) is not involved in binding of κ-PVIIA, we consider only the pore domain (S5−P−S6) of the channel models, which corresponds to residues 376−489 of Shaker, 306−419 of Kv1.1, and 308−421 of Kv1.2. Alignment of the Shaker and Kv1 sequences in the pore domain reveals 88% identity. The residues that differ between Shaker and Kv1 are indicated in the alignment diagram (Table 1). Note that almost all the functional mutations occur in the extracellular interface. In Shaker, these correspond to residues 420−427 (turret) and 449−454 (extended region outside the selectivity filter). Because both Shaker and Kv1 channels have exactly 114 residues in the pore domain, homology models for Shaker and Kv1.1 are easily constructed from the Kv1.2 structure using the mutator plugin in VMD.[46] We have checked the quality of the homology models using QMEAN6 and *Z* score from Swiss Model.[47] The Shaker model results for both scores are within 98% of those of Kv1.2, and the Kv1.1 model results are within 78% of those of Kv1.2.

Before docking κ-PVIIA, we performed MD simulations for all three channel models to ensure that they have stable side chain configurations. For this purpose, we used the protocols established in previous MD simulations of potassium channels.[48,49] Briefly, channel proteins are embedded in a POPE bilayer and solvated with a 100 mM KCl solution. First the protein is fixed, and the system is equilibrated with pressure coupling until the correct lipid and water densities are obtained. This is followed by gradual relaxation of the protein side chain and backbone atoms under pressure coupling in the *z* direction with the *x*−*y* dimensions of the box fixed. After equilibration, each system is run for 5 ns for analysis. The rmsd's obtained from the trajectory data confirm that each channel model has a stable structure and its backbone follows closely that of the structure of PDB entry 2R9R.

In constructing the homology models, we have paid special attention to the possibility of intra- and interdomain linking among the mutated residues. This was an important issue in modeling of the Kv1.3 channel, where H404 (corresponding to V381 in Kv1.2) and D402 side chains were found to be cross-linked.[34] The residues corresponding to V381 in Kv1.2 are Y379 in Kv1.1 and T449 in Shaker (Table 1). Both have a hydroxyl group and, in principle, can make a cross-link with the corresponding D377 (Kv1.1) and D447 (Shaker) side chains. However, the cross-linking of T449 and D447 is observed only in Shaker simulations (see Figure S1 of the Supporting Information for a snapshot of the cross-link and Figure S2 of the Supporting Information for the time series of T449−D447 distances). The Tyr side chains are presumably too bulky to fit around the filter, which prevents Y379−D377 cross-linking in Kv1.1. As will be shown in Results and Discussion, a correct description of the T449−D447 cross-linking in Shaker is essential for obtaining an accurate model of the Shaker−κ-PVIIA complex. Conversely, the presence of the bulky Y379 side chain outside the filter periphery in Kv1.1 obstructs formation of close contacts between the channel and toxin residues. Another intradomain link that is specific to Shaker occurs between the side chains of K427 and D431. While these residues are not directly involved in toxin binding, their mutation disrupts the binding site, resulting in observable effects.

Modeling of K^+ Channel−κ-PVIIA Complexes. κ-PVIIA is a 27-residue peptide with a CRIONQKCFQHLDDCCSR-KCNRFNKCV sequence. NMR structures of κ-PVIIA (20 conformers) are available from the PDB (entry 1AV3).[35] A snapshot of κ-PVIIA depicting the important residues involved in binding to Shaker is shown in Figure 1. The structure of κ-PVIIA is stabilized by three disulfide bonds (C1−C16, C8−C20, and C15−C26),[35,36] the side chain H-bond between Q10 and N24, and the side chain−carbonyl oxygen coupling

dx.doi.org/10.1021/bi301257p | *Biochemistry* 2013, 52, 1631−1640

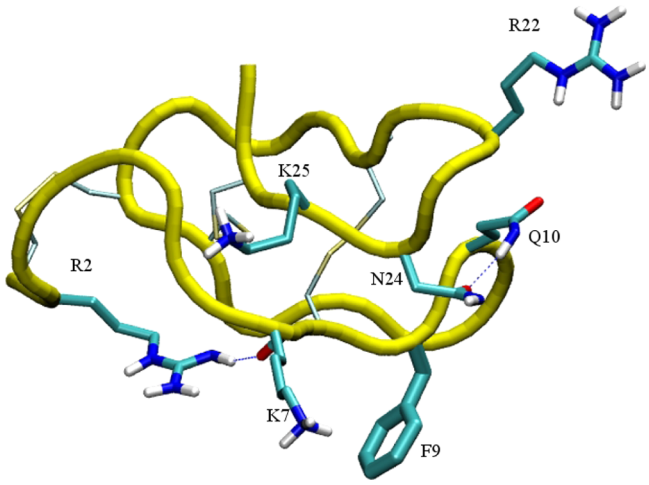

Figure 1. NMR structure of κ-PVIIA showing the important residues involved in binding to Shaker (R2, K7, F9, and K25). Three disulfide bonds (C1−C16, C8−C20, and C15−C26) as well as R2−K7 and Q10−N24 bonds are shown.

between R2 and K7. It is seen from Figure 1 that there are no disulfide bonds to stabilize the turn between R22 and N24, and this role is taken over by the Q10−N24 H-bond (see Figure S3 of the Supporting Information for time series of the Q10−N24 distances). As discussed further below, disruption of the Q10−N24 bond via mutations leads to a shape change, which affects the binding mode of κ-PVIIA.

Initial complex structures of the potassium channels with κ-PVIIA are generated using HADDOCK,[50,51] which has been shown to give good results for docking of toxins to ion channels.[34,52] All 20 NMR conformers of κ-PVIIA are used for docking to obtain an adequate sampling of the side chain orientations. Because K7 has been identified as the pore inserting Lys in experiments,[36,37] we use the proximity of the K7 side chain to the filter Tyr (Y445 in Shaker, Y375 in Kv1.1, and Y377 in Kv1.2) as a restraint in HADDOCK calculations. Several hundred complexes are created for each channel and sorted on the basis of their energy scores. For each group of channel−κ-PVIIA complexes, the top 10 are analyzed and checked against the available experimental information. The overall features of all the analyzed complexes are found to be very similar, and therefore, the one with the best energy score is selected for refinement with MD simulations.

Each channel−κ-PVIIA complex structure obtained from docking is aligned with the corresponding channel model in the membrane, and the coordinates of the toxin are transferred to the channel model. The complex structures are then relaxed in the MD simulation according to the established protocols mentioned above. After equilibration, each complex is simulated for 20 ns, and the last 15 ns of the trajectory data is used for analysis of the binding mode. During these MD simulations, a small restraint with a k of 0.1 kcal mol^{-1} Å^{-2} is applied to the channel backbone atoms to preserve the integrity of the channel, but no restraints are imposed on the toxin.

MD Simulations and Free Energy Calculations. MD simulations in this study are performed using version 2.7 of NAMD[53] with the CHARMM27 force field,[54] including the CMAP correction.[55] An NpT ensemble is used with periodic boundary conditions. The pressure is kept at 1 atm and the temperature at 300 K using Langevin coupling with damping coefficients of 5 ps^{-1}. Lennard-Jones interactions are switched off smoothly within a distance of 10−13.5 Å. Electrostatic interactions are computed without truncation using the particle mesh Ewald algorithm. A time step of 2 fs has been used in all MD simulations. The trajectory data are written at 5 ps intervals, except in umbrella sampling simulations where the reaction coordinate is written at every time step.

The potential of mean force (PMF) for dissociation of κ-PVIIA from Shaker is constructed using umbrella sampling MD simulations. As the method has been described in detail previously,[27,28] we give a brief description here. The reaction coordinate is chosen as the distance between the centers of mass (COM) of the channel and the toxin along the channel axis. Initially, 31 umbrella windows are created along the channel axis at 0.5 Å intervals using steered MD with a force constant k of 30 kcal mol^{-1} Å^{-2} and a speed v of 5 Å/ns. The same force constant is used in umbrella sampling simulations, which is found to be optimal for toxins of this size.[28] After the overlaps of the neigboring distributions had been checked, two more windows were included between windows 5 and 6 and windows 8 and 9, where the overlap dropped below 5%. We have also extended the simulations by six more windows to ensure that the PMF has flattened out in the bulk region. The reaction coordinates collected from the simulations are unbiased and combined using the weighted histogram analysis method.[56] Each window is simulated for 5 ns, which is found to be sufficient to obtain a converged PMF. A similar protocol is used in constructing the PMF for dissociation of κ-PVIIA from Kv1.2.

The binding constant is determined from a one-dimensional integral of the PMF, $W(z)$, along the z axis[28]

$$K_{eq} = \pi R^2 \int_{z_1}^{z_2} e^{-W(z)/k_B T}\, dz \quad (1)$$

where z_1 and z_2 are the initial and final points in the PMF, respectively, and πR^2 is the average cross sectional area of the binding pocket as explored by the COM of the toxin, which is determined from its transverse fluctuations. The value of R is obtained from restraint free MD simulations of the toxin in the binding pocket: 0.70 Å for Shaker and 0.64 Å for Kv1.2. Finally, the standard binding free energy of κ-PVIIA is determined from the binding constant using

$$\Delta G_b = -k_B T \ln(K_{eq} C_0) \quad (2)$$

where C_0 is the standard concentration of 1 M (i.e., $1/C_0$ = 1661 Å^3).

The effect of toxin mutations on the binding energy is studied using the free energy perturbation (FEP) method. From the thermodynamic cycle, the change in the binding free energy due to a mutation is given by

$$\Delta\Delta G_b = \Delta G_b(\text{mut}) - \Delta G_b(\text{wt}) = \Delta G^{\text{site}}(\text{wt} \rightarrow \text{mut}) + \Delta G^{\text{bulk}}(\text{mut} \rightarrow \text{wt}) \quad (3)$$

where wt and mut refer to the wild type and mutated form of the toxin, respectively. As long as the mutations do not cause any changes in the binding mode, the FEP calculations in eq 3 can be performed simultaneously in the binding site and bulk in opposite directions to obtain the required binding free energy difference, $\Delta\Delta G_b$. FEP calculations are performed using 52 windows with a 40 ps equilibration and a 40 ps production time in each window, which is found to be adequate for charge neutral mutations considered here.

dx.doi.org/10.1021/bi301257p | *Biochemistry* 2013, 52, 1631−1640

RESULTS AND DISCUSSION

Characterization of the Shaker−κ-PVIIA Complex. There are ample mutagenesis data for the binding of κ-PVIIA to Shaker,[37] which we use to validate our complex model. Snapshots of the Shaker−κ-PVIIA complex obtained after refinement with MD simulations are shown in Figure 2. To give a more quantitative account of the binding mode, we list in Table 2 the pairs of residues involved in binding and the average distances between the pairs of atoms. The average atomic distances are obtained from 15 ns MD simulations of the equilibrated complex. Because the proximity of atoms alone is not sufficient to assess their coupling strength, we use the persistence of the pair distance while the toxin is pulled out as a measure of their strength. The average pair distances, determined from umbrella sampling MD simulations, are plotted as a function of the toxin COM in Figure 3. Inspecting Table 2 and Figure 3, one can identify K7, F9, and R2 as the most strongly coupled residues on κ-PVIIA, which is in good agreement with the mutagenesis data.[37] K7 is the pore-inserting lysine, whose side chain makes H-bonds with the carbonyls of the filter Y445 residues. The K7−Y445 contact is seen to persist up to 4 Å pulling of κ-PVIIA, which demonstrates its strength. The K7A mutation abolishes this charge contact, leading to a >900-fold increase in IC_{50}.[37] The conservative K7R mutation results in a similar increase in IC_{50}, but this is due to the inability of the arginine side chain to enter the filter. Our results indicate that hydrophobic F9−F425 coupling is a similarly strong interaction; the side chain of F9 is perpendicular to the side chain of F425, and the coupling persists for almost 5 Å. This coupling is abolished by the F9A mutation but not by the conservative F9Y mutation, consistent with the mutagenesis data. The R2−D447 charge interaction is predicted to be slightly weaker than the other two because both the contact distance and its slope in Figure 3 are slightly larger. The mutagenesis data do not distinguish between the R2A and R2K mutations, resulting in a >900-fold increase in IC_{50} in both cases. The effect of the former mutation is obvious, and the latter is explained by the fact that the R2−K7 bond in κ-PVIIA is broken after the R2K mutation; the K2 side chain is too distant to make a contact with the D447 carbonyl oxygen.

The next three residues involved in binding (F23, N24, and K25) have longer contact distances and dissociate relatively earlier, indicating an intermediate-strength coupling. The K25A mutation results in a >100-fold increase in IC_{50}, while the F23A and N24A mutations increase IC_{50} by <20-fold.[37] Here K25 exhibits some interesting behavior. Its side chain forms a charge contact with the side chain of D447 (with the carboxyl oxygen that is not involved in cross-linking) and another contact with the side chain of N423. The distances in Table 2 may suggest that the K25−N423 interaction is the stronger interaction, but from the persistence of the contact distances in Figure 3, one clearly identifies the K25−D447 interaction as the stronger

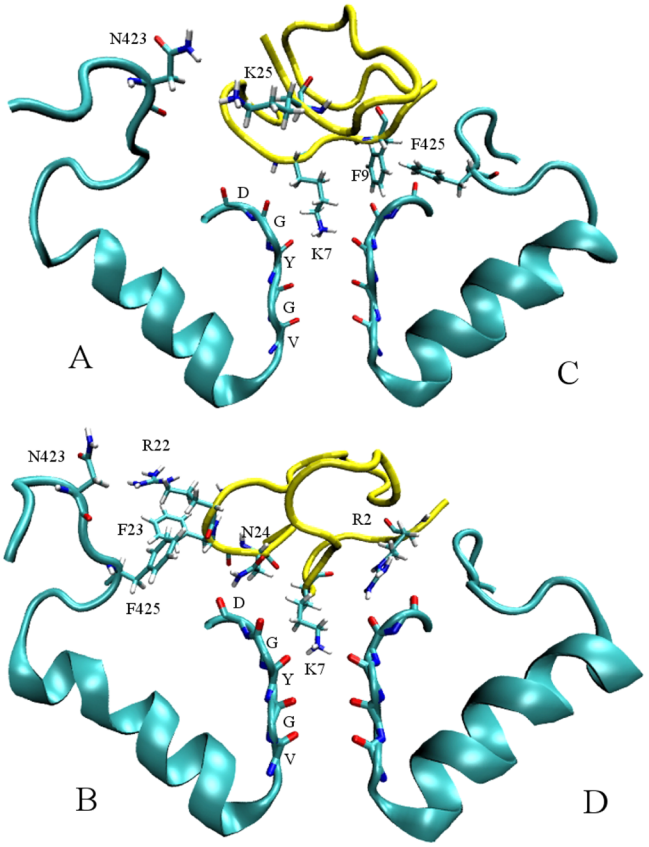

Figure 2. Snapshots of the Shaker−κ-PVIIA complex showing the important residues involved in binding. To give a full picture of the binding mode, we provide two cross sections of the complex showing monomers A and C (top) and monomers B and D (bottom) separately.

Table 2. Strongly Interacting Residues in the Channel−Toxin Complexes[a]

κ-PVIIA−Shaker	average distance	κ-PVIIA−Kv1.1	average distance	κ-PVIIA−Kv1.2	average distance
R2(N_1)−D447(O)D	3.9 ± 0.4	R2(N_2)−D377(O)A	5.0 ± 0.7	R2(N_2)−D379(O)D	3.7 ± 0.5
Q6(N_1)−D447(O)A	4.7 ± 0.3	Q6(N_1)−D377(O)A	5.1 ± 0.9	Q6(N_1)−D379(O)A	3.2 ± 0.3
K7(N_1)−Y445(O)ABC	2.7 ± 0.2	K7(N_1)−Y375(O)ABC	2.8 ± 0.3	K7(N_1)−Y377(O)ABC	2.7 ± 0.2
F9(C_ζ)−T449($C_{\gamma 2}$)C	4.4 ± 0.3	F9($C_{\delta 2}$)−Y379($C_{\varepsilon 2}$)C	3.9 ± 0.3	F9($C_{\varepsilon 1}$)−V381($C_{\gamma 1}$)C	4.7 ± 0.6
F9(Benz)−F425(C_ζ)C	3.6 ± 0.2				
R22(N_1)−N423(O_1)B	6.2 ± 1.4	R22(N_2)−E351(O_2)B	3.0 ± 1.0	R22(N_2)−D355(O_1)B	3.5 ± 1.3
F23(Benz)−F425(C_ζ)B	5.0 ± 0.8				
N24(N_1)−D447(O)B	3.0 ± 0.4	N24(N_1)−D377(O)C	3.8 ± 0.5	N24(N_1)−D379(O)C	2.9 ± 0.3
K25(N_1)−D447(O_1)B	6.1 ± 1.4	K25(N_1)−Y379(O_1)A	4.7 ± 1.0	K25(N_1)−D379(O)B	2.9 ± 0.6
K25(N_1)−N423(O_1)A	5.0 ± 1.3				

[a]The average distances between the atoms are calculated from the MD simulations (in angstroms). The N−O distances are shown for the charge interactions and the shortest C−C distances for the hydrophobic ones. Bare C, N, and O refer to the backbone atoms, and those with subscripts refer to the side chain atoms. The monomer identity is given at the end of the residue number. For the filter Y residues, the average of the three N−O distances is given. Benz refers to the COM of the benzyl group.

dx.doi.org/10.1021/bi301257p | Biochemistry 2013, 52, 1631−1640

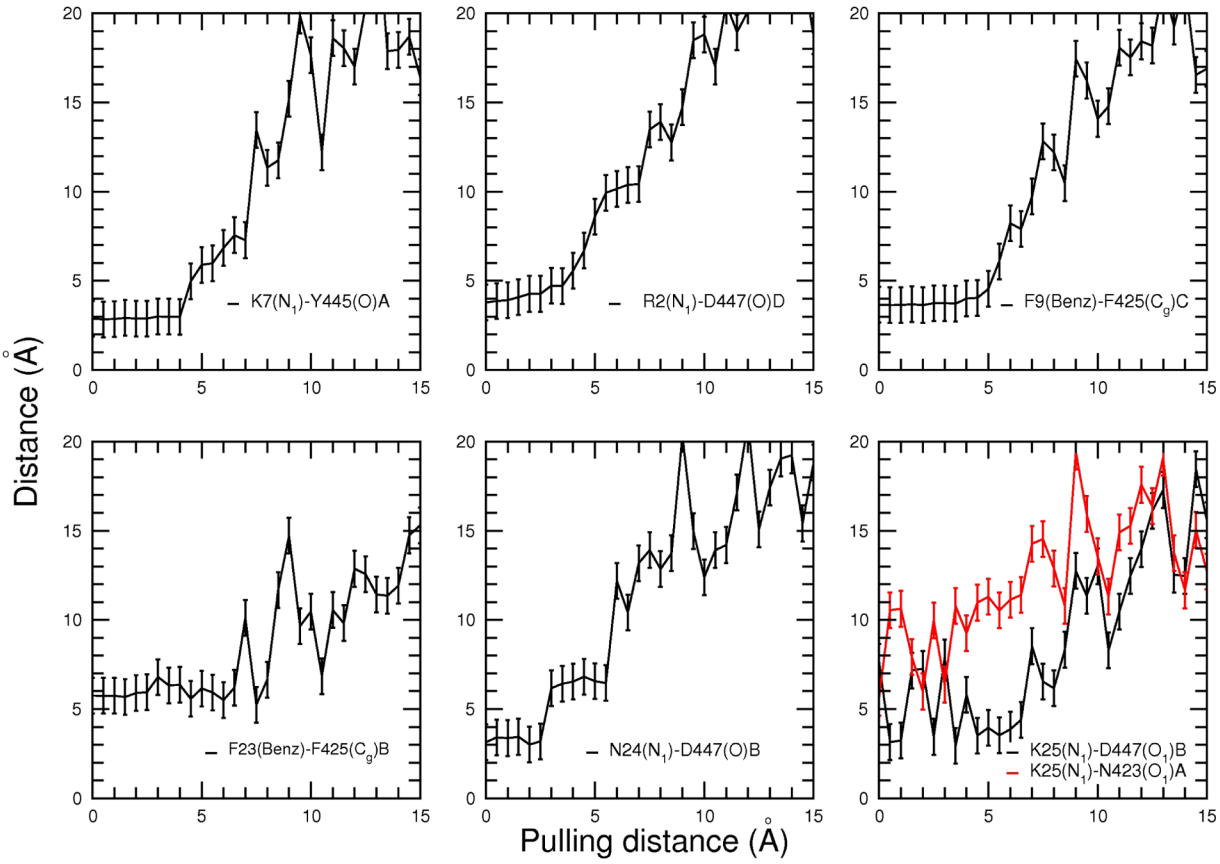

Figure 3. Change in the average pair distances with pulling distance of κ-PVIIA from Shaker. Only the most important pairs in Table 2 are shown. The average distances are obtained from the trajectory data used in the construction of the final PMF in Figure 5. Error bars indicate one standard deviation.

interaction. Finally, we mention Q6 and R22, which have relatively large pair distances that remain large as the toxin is pulled out, indicating their weakness. Their mutation results in smaller increases in IC_{50} consistent with this interpretation.

There are also mutation data on several channel residues.[23,37] The T449Y and T449K mutations make the channel insensitive to 1 μM κ-PVIIA,[23] which is explained by the breaking of the T449−D447 cross-link. The mutated side chains are too large to fit around the filter and project out of the filter, disrupting the important hydrophobic interactions involving F9 and F23. This is depicted in Figure 4, which provides a more detailed picture of how the F9−F425 coupling is related to the T449−D447 cross-linking. Most of the mutations considered in ref 37 do not involve the residues identified in Table 2, and not surprisingly, most of them have a negligible effect on IC_{50}. The ones that have a measurable effect do so indirectly by disrupting the binding mode. For example, the D431K mutation breaks the K427−D431 bond, and the released K431 side chain interferes with the binding of κ-PVIIA. Similarly, the K427D mutation releases the D431 side chain, which slightly increases the κ-PVIIA affinity. In the S424K mutation, the K424 side chain interferes with the hydrophobic F9−F425 interaction, reducing the κ-PVIIA affinity. Only three of the mutations involve the residues listed in Table 2.[37] The F425Y and N423K mutations cause little change in IC_{50} because the former is a conservative mutation and the latter has a weak interaction with R22. The T449S mutation is also a conservative mutation, but it does have some effect on IC_{50}. We see from Table 2 that the

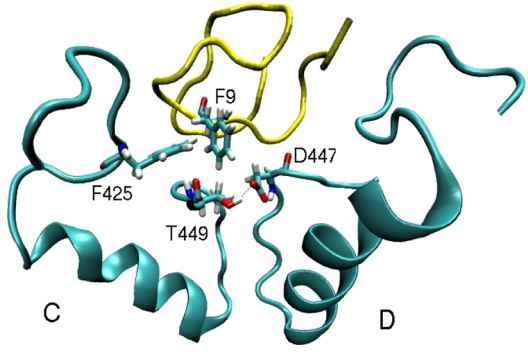

Figure 4. Alternative view of the Shaker−κ-PVIIA complex that demonstrates the importance of the T449−D447 cross-linking in preserving the strong F9−F425 hyrophobic interaction. The T449Y mutation introduces a bulky side chain that projects out of the filter and disrupts this interaction.

side chain carbon of T449 has a hydrophobic interaction with F9, which explains why its mutation to S449 reduces affinity.

It is instructive to compare the Shaker−κ-PVIIA complex obtained here with an earlier model, in which the T449−D447 cross-linking in Shaker is not taken into account.[44] As a result, the T449 side chains project out of the filter and distort the docking of toxin, resulting in a binding mode very different from that found here. For example, R18 and E422B, and R22 and E422D (instead of R2−D447), are predicted to make contact and have strong interactions, which are not observed in the mutagenesis data.[37] Apart from the functional dyad (K7 and

dx.doi.org/10.1021/bi301257p | Biochemistry 2013, 52, 1631−1640

F9), none of the interactions proposed in ref 44 match the ones listed in Table 2, which have been shown to agree with the mutagenesis data. This underscores the importance of correct modeling of the homologues of ion channels in toxin binding studies.

Free Energy Calculations. The PMF for the dissociation of κ-PVIIA from Shaker is determined from the umbrella sampling MD simulations as described in Methods. Convergence of the PMF is checked from block data analysis, and the final PMF is shown to converge well (see Figure S4 of the Supporting Information). The stability of the toxin during the umbrella sampling simulations is also a concern.[28] We have checked the stability of κ-PVIIA by comparing its average rmsd obtained from each umbrella window to the bulk rmsd (Figure S5 of the Supporting Information). This study shows that the toxin preserves its shape in the binding site and in the bulk region while undergoing slight changes between those sites. The final PMF is shown in Figure 5. To gain some insight, we identify three regions in the PMF and correlate them with the pair distances shown in Figure 3.

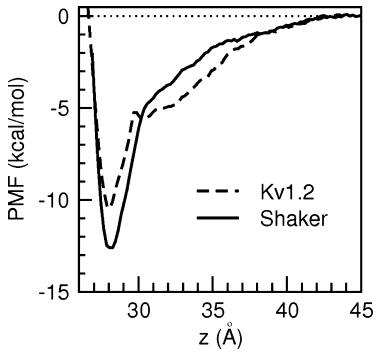

Figure 5. PMFs for dissociation of κ-PVIIA from Shaker and Kv1.2. In both cases, the binding site is ∼28 Å (z) from the COM of the channels and the bulk region is reached at ∼43 Å (z).

(1) In the binding pocket (0−2.5 Å pulling distance), all of the contact distances between the pairs are preserved and κ-PVIIA remains tightly bound to the channel. As the COM of κ-PVIIA is pulled away, the side chains involved in binding have to stretch to keep contact, which results in a steep increase in the PMF.

(2) In the transition region (2.5−7 Å pulling distance), contacts are gradually broken in the following order: N24, R2, K7, F9, and F23. The PMF still increases but not as sharply as in the binding pocket because the energy from stretching is returned when the contacts are broken.

(3) In the electrostatic region (7−16 Å pulling distance), there are no contacts left and the toxin interacts with the channel residues via the screened Coulomb interaction only, which is responsible for the shoulder in the PMF. Large fluctuations in the pair distances indicate that the toxin is more or less to free to rotate.

Using eq 1, we numerically integrate the PMF to find the binding constant and then determine the standard binding free energy from eq 2. The calculated value (G_b = −8.9 kcal/mol) is in good agreement with the experimental value of −9.8 kcal/mol, determined from the IC_{50} measurements.[22,37] This provides further support for the accuracy of the proposed model of the Shaker−κ-PVIIA complex.

We have also performed free energy perturbation calculations to provide a more quantitative comparison of the model results with the mutagenesis data. Because it is difficult to obtain convergence in FEP calculations involving charge mutations, we have focused on neutral ones. Specifically, we have considered the F9A and F23A mutations. Unfortunately, the F9A mutation is observed to break the Q10−N24 bond, resulting in a change in the shape of the toxin, which makes the FEP calculation impractical in this case as well (see Figures S3 and S6 of the Supporting Information). The F23A mutation does not cause any change in shape in κ-PVIIA, and the FEP calculation is feasible. Using eq 3, we have calculated the change in the binding free energy due to F23A ($\Delta\Delta G_b$) and obtained a value of 2.7 kcal/mol in the forward direction and a value of −2.0 kcal/mol in the backward direction. This shows that hysteresis effects are within the fluctuations. Taking the average of the forward and the negative of the backward values yields a $\Delta\Delta G_b$ of 2.35 kcal/mol, which is in good agreement with the experimental value of 1.7 kcal/mol.[37]

Complexes of κ-PVIIA with Kv1.1 and Kv1.2. To understand why κ-PVIIA binds to Shaker with a nanomolar affinity while Kv1 channels remain insensitive to it, we compare the binding modes of the respective complexes. Snapshots of the Kv1.1−κ-PVIIA and Kv1.2−κ-PVIIA complexes are shown in Figures 6 and 7, respectively. Pair distances for the residues involved in binding are provided in Table 2. Inspection of the pairs of residues in Table 2 and the complex structures in Figures 2, 6, and 7 shows that there is a quite good overlap

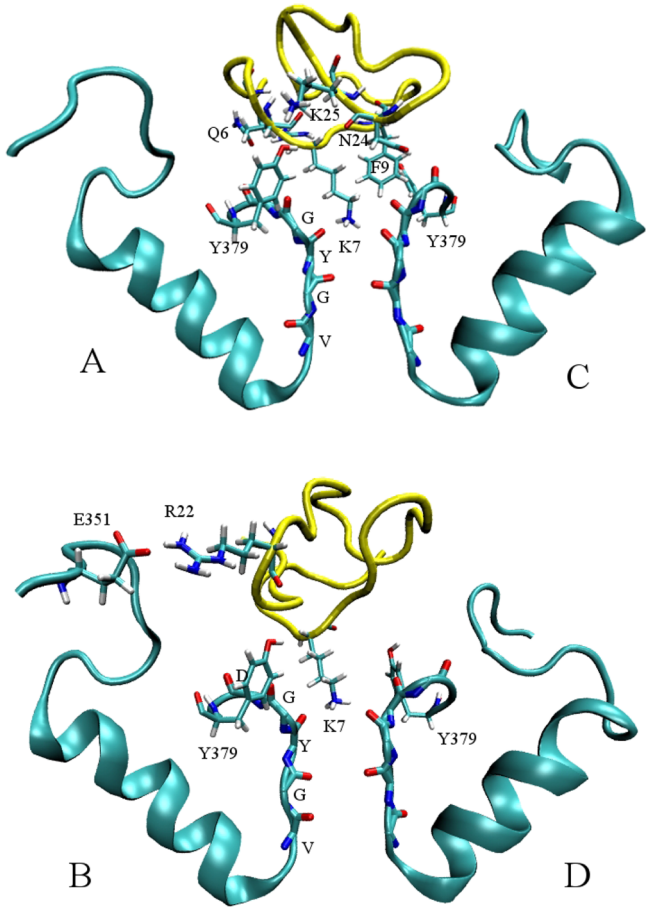

Figure 6. Same as Figure 2 but for the Kv1.1−κ-PVIIA complex.

dx.doi.org/10.1021/bi301257p | Biochemistry 2013, 52, 1631−1640

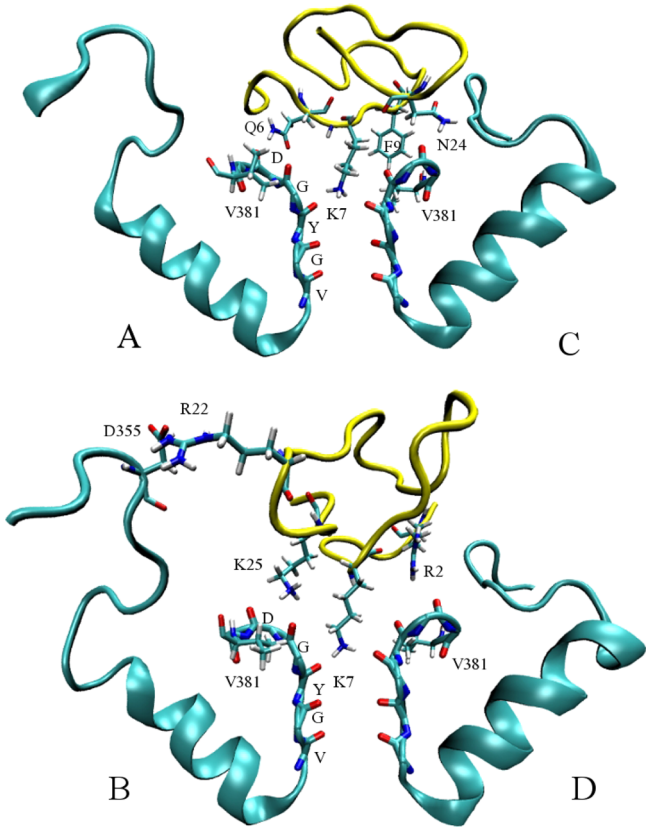

Figure 7. Same as Figure 2 but for the Kv1.2–κ-PVIIA complex.

among the charge interactions but not the hydrophobic ones. There are no counterparts in the Kv1.1 and Kv1.2 complexes for the pair of hydrophobic interactions (F9–F425C and F23–F425B) that have been shown to play an important role in the binding of κ-PVIIA to Shaker. From Table 1, it is seen that F425 is replaced by H355 in Kv1.1 and Q357 in Kv1.2, and neither is involved in any strong interactions with κ-PVIIA. Thus, we identify the mutation of F425 in Shaker as the main reason for the insensitivity of Kv1 channels to κ-PVIIA. This is supported by the experiments with the F425G mutation in Shaker, which abolishes κ-PVIIA sensitivity.[23]

To quantify these observations, we construct the PMF for the dissociation of κ-PVIIA from Kv1.2 (dashed line in Figure 5). Evidence of the convergence of the PMF is provided in Figure S7 of the Supporting Information. The Kv1.2 PMF is ∼2.5 kcal/mol shallower than that of Shaker, which gives an estimate of the contribution of the hydrophobic interactions in the Shaker–κ-PVIIA complex. The standard binding free energy (G_b) is determined from the PMF to be −6.5 kcal/mol, which is consistent with the limit set from the experimental binding constant measurements of greater than −8 kcal/mol.[22,23] More insights into the dissociation process can be gathered by inspecting the evolution of the pair distances with the pulling distance of the toxin (Figure 8). All the contacts between the pairs except R22 and K25 are broken by an ∼3 Å distance, which correlates with the rapid increase in the PMF. From 3 to 10 Å, the toxin remains anchored to Kv1.2 via the contacts of R22 and K25 with the domain B residues (see Figure 7). After that, there are no contacts left and the toxin interacts with the channel via the long-range Coulomb interaction.

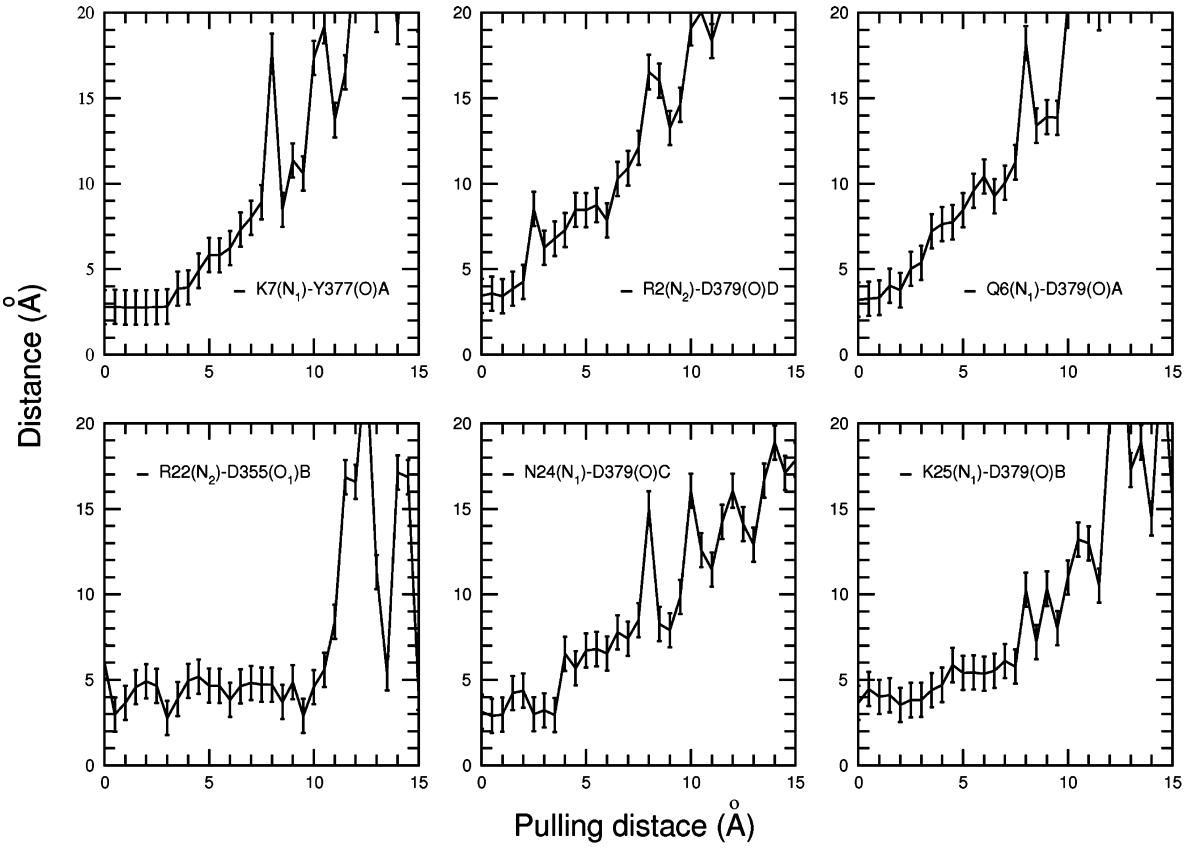

Figure 8. Same as Figure 3 but for the Kv1.2–κ-PVIIA complex.

dx.doi.org/10.1021/bi301257p | *Biochemistry* 2013, 52, 1631–1640

While the charge interactions exhibit almost 1:1 correspondence between the Shaker and Kv1.2 complexes, some differences arise when these two are compared to the Kv1.1 complex. This again highlights the disruptive effect of the Y379 side chains in Kv1.1, which project out of the filter (recall that the T449Y mutation in Shaker has a similar effect on the binding of κ-PVIIA). We can infer from Table 2 that the natural partners of R2 and K25 in Kv1.1 would be D377(O)D and D377(O)B, respectively, but this is thwarted by the presence of the Y379 side chains; R2 and K7 instead make inferior contacts with the residues in the neighboring monomers. On the basis of this observation, we predict the affinity of κ-PVIIA for Kv1.1 to be even lower than its affinity for Kv1.2. Because Kv1.1 is involved in the central nervous system, it is often an undesired target for potential drugs developed for other Kv1 channels, and much effort goes into finding analogues that have reduced affinity for Kv1.1.[14] The insights gathered from this study indicate that binding to Kv1.1 can occur through only charge interactions. Thus, one way of achieving selectivity against Kv1.1 is to construct analogues with hydrophobic residues placed at appropriate places that disrupt the existing charge interactions.

■ CONCLUSIONS

We have presented a computational study of binding of κ-PVIIA toxin to the *Drosophila* Shaker and Kv1 channels. Our results provide a rationalization for the experimental results that reveal that κ-PVIIA binds to Shaker with high affinity but not to the Kv1 channels, despite the fact that they also belong to the Shaker family. Detailed analysis of the binding modes shows that the hydrophobic interactions emanating from F425 in Shaker are the main reason for its sensitivity to κ-PVIIA, and its mutation to hydrophilic residues in Kv1 channels renders them insensitive to κ-PVIIA. Thus, one has to be extra cautious in generalizing the ligand binding results obtained from Shaker with the Kv1 channels.

The Shaker−κ-PVIIA complex constructed using docking and MD simulations has been validated using the extensive mutagenesis data available as well through the binding free energy of κ-PVIIA, and good agreement have been obtained in both cases. The chemical accuracy of 1 kcal/mol obtained for the binding free energy here has also been attained in several other binding free energy calculations of channel−toxin complexes where the structure has been either known from experiments[28] or validated from mutagenesis data.[34] The ability of the simulation methods used in these studies to yield accurate complex models and binding free energies is very encouraging, and one hopes that they will be used more extensively in future studies of protein−ligand interactions. In particular, these methods would be very useful in solving structure-based ligand design problems.

■ ASSOCIATED CONTENT

Supporting Information

Six figures showing the stability of the toxin and convergence of the PMF. This material is available free of charge via the Internet at http://pubs.acs.org.

■ AUTHOR INFORMATION

Corresponding Author

*School of Physics, University of Sydney, Sydney, New South Wales 2006, Australia. Telephone: +61 2 9036 5306. E-mail: serdar@physics.usyd.edu.au.

Funding

This work was supported by grants from the Australian Research Council. Calculations were performed at the National Computational Infrastructure (Canberra, Australia), which is supported by the Australian Commonwealth Government.

Notes

The authors declare no competing financial interest.

■ ABBREVIATIONS

COM, center of mass; κ-PVIIA, κ-conotoxin PVIIA; Kv1, Shaker family of voltage-gated potassium channels; MD, molecular dynamics; PMF, potential of mean force; rmsd, root-mean-square deviation; Shaker, *Drosophila* Shaker K^+ channel.

■ REFERENCES

(1) Hille, B. (2001) *Ionic Channels of Excitable Membranes*, 3rd ed., Sinauer Associates, Sunderland, MA.
(2) Gutman, G. A., Chandy, K. G., Grissmer, S., Lazdunski, M., McKinnon, D., Pardo, L. A., Robertson, G. A., Rudy, B., Sanguinetti, M. C., Sthmer, W., and Wang, X. (2005) International Union of Pharmacology. LIII. Nomenclature and molecular relationships of voltage-gated potassium channels. *Pharmacol. Rev. 57*, 473−508.
(3) Mert, T. (2007) Kv1 channels in signal conduction of myelinated nerve fibers. *Rev. Neurosci. 17*, 369−374.
(4) Terlau, H., and Olivera, B. M. (2004) Conus venoms: A rich source of novel ion channel-targeted peptides. *Physiol. Rev. 84*, 41−68.
(5) Rodriguez de la Vega, R. C., and Possani, L. D. (2004) Current views on scorpion toxins specific for K^+-channels. *Toxicon 43*, 865−875.
(6) Mouhat, S., Andreotti, N., Jouirou, B., and Sabatier, J. M. (2008) Animal toxins acting on voltage-gated potassium channels. *Curr. Pharm. Des. 14*, 2503−2518.
(7) MacKinnon, R., and Miller, C. (1989) Mutant potassium channels with altered binding of charybdotoxin, a pore blocking peptide inhibitor. *Science 245*, 1382−1385.
(8) Hidalgo, P., and MacKinnon, R. (1995) Revealing the architecture of a K^+ channel pore through mutant cycles with a peptide inhibitor. *Science 268*, 307−310.
(9) Duterte, S., and Lewis, R. J. (2010) Use of venom peptides to probe ion channel structure and function. *J. Biol. Chem. 285*, 13315−13320.
(10) Lewis, R. J., and Garcia, M. L. (2003) Therapeutic potential of venom peptides. *Nat. Rev. Drug Discovery 2*, 790−802.
(11) Wulff, H., Castle, N. A., and Pardo, L. A. (2009) Voltage-gated potassium channels as therapeutic targets. *Nat. Rev. Drug Discovery 8*, 982−1001.
(12) Twede, V. D., Miljanich, G., Olivera, B. M., and Bulaj, G. (2009) Neuroprotective and cardioprotective conopeptides: An emerging class of drug leads. *Curr. Opin. Drug Discovery Dev. 12*, 231−239.
(13) Beeton, C., Wulff, H., Standifer, N. E., Azam, P., Mullen, K. M., Pennington, M. W., Kolski-Andreaco, A., Wei, E., Grino, A., Counts, D. R., et al. (2006) Kv1.3 channels are a therapeutic target for T cell-mediated autoimmune diseases. *Proc. Natl. Acad. Sci. U.S.A. 103*, 17414−17419.
(14) Chi, V., Pennington, M. W., Norton, R. S., Tarcha, E. J., Londono, L. M., Sims-Fahey, B., Upadhyay, S. K., Lakey, J. T., Iadonato, S., Wulff, H., et al. (2012) Development of a sea anemone toxin as an immunomodulator for therapy of autoimmune diseases. *Toxicon 59*, 529−546.
(15) Norton, R. S. (2010) μ-Conotoxins as leads in the development of new analgesics. *Molecules 15*, 2825−2844.
(16) Clare, J. J. (2010) Targeting voltage-gated sodium channels for pain therapy. *Expert Opin. Invest. Drugs 19*, 45−62.
(17) Livett, B. G., Sandall, D. W., Keyas, D., Down, J., Gayler, K. R., Satkunanathan, N., and Khalil, Z. (2006) Therapeutic applications of

conotoxins that target the neuronal nicotinic acetylcholine receptor. *Toxicon 48*, 810−829.
(18) Carstens, B. B., Clark, R. J., Daly, N. L., Harvey, P. J., Kaas, Q., and Craik, D. J. (2011) Engineering of conotoxins for the treatment of pain. *Curr. Pharm. Des. 17*, 4242−4253.
(19) Tempel, B. L., Papazian, D. M., Schwarz, T. L., Jan, Y. N., and Jan, L. Y. (1997) Sequence of a probable potassium channel component encoded at Shaker locus of *Drosophila*. *Science 237*, 770−775.
(20) Kamb, A., Iverson, L. E., and Tanouye, M. A. (1987) Molecular characterization of Shaker, a *Drosophila* gene that encodes a potassium channel. *Cell 50*, 405−413.
(21) Shealy, R. T., Murphy, A. D., Ramarathnam, R., Jakobsson, E., and Subramaniam, S. (2003) Sequence-function analysis of the K^+-selective family of ion channels using a comprehensive alignment and the KcsA channel structure. *Biophys. J. 84*, 2929−2942.
(22) Terlau, H., Shon, K. J., Grilley, M., Stocker, M., Sthmer, W., and Olivera, B. M. (1996) Strategy for rapid immobilization of prey by a fish-hunting marine snail. *Nature 381*, 148−151.
(23) Shon, K. J., Stocker, M., Terlau, H., Sthmer, W., Jacobsen, R., Walker, C., Grilley, M., Watkins, M., Hillyard, D. R., Gray, W. R., and Olivera, B. M. (1998) κ-Conotoxin PVIIA is a peptide inhibiting the Shaker K^+ channel. *J. Biol. Chem. 273*, 33−38.
(24) Ferber, M., Sporning, A., Jeserich, G., DeLaCruz, R., Watkins, M., Olivera, B. M., and Terlau, H. (2003) A novel conus peptide ligand for K^+ channels. *J. Biol. Chem. 278*, 2177−2183.
(25) Ferber, M., Al-Sabi, A., Stocker, M., Olivera, B. M., and Terlau, H. (2004) Identification of a mammalian target of M-conotoxin RIIIK. *Toxicon 43*, 915−921.
(26) Alonso, H., Bliznyuk, A. A., and Gready, J. E. (2006) Combining docking and molecular dynamic simulations in drug design. *Med. Res. Rev. 26*, 531−568.
(27) Chen, P. C., and Kuyucak, S. (2009) Mechanism and energetics of charybdotoxin unbinding from a potassium channel from molecular dynamics simulations. *Biophys. J. 96*, 2577−2588.
(28) Chen, P. C., and Kuyucak, S. (2011) Accurate determination of the binding free energy for KcsA-Charybdotoxin complex form a the potential of mean force calculations with restraints. *Biophys. J. 100*, 2466−2474.
(29) Yu, L. P., Sun, C. H., Song, D. Y., Shen, J. W., Xu, N., Gunasekera, A., Hajduk, P. J., and Olejniczak, E. T. (2005) Nuclear magnetic resonance structural studies of a potassium channel-charybdotoxin complex. *Biochemistry 44*, 15834−15841.
(30) Yi, H., Qiu, S., Cao, Z. J., Wu, Y. L., and Li., W. X. (2008) Molecular basis of inhibitory peptide maurotoxin recognizing Kv1.2 channel explored by ZDOCK and molecular dynamic simulations. *Proteins 70*, 844−854.
(31) Khabiri, M., Nikouee, A., Cwiklik, L., Grissmer, S., and Ettrich, R. (2011) Charybdotoxin unbinding from the mKv1.3 potassium channel: A combined computational and experimental study. *J. Phys. Chem. B 115*, 11490−11500.
(32) Chen, R., Robinson, A., Gordon, D., and Chung, S. H. (2011) Modeling the binding of three toxins to the voltage-gated potassium channel (Kv1.3). *Biophys. J. 101*, 2652−2660.
(33) Chen, R., and Chung, S. H. (2012) Binding modes of μ-conotoxin to the bacterial sodium channel (NavAb). *Biophys. J. 102*, 483−488.
(34) Rashid, M. H., and Kuyucak, S. (2012) Affinity and selectivity of ShK toxin for the Kv1 potassium channels from free energy simulations. *J. Phys. Chem. B 116*, 4812−4822.
(35) Scanlon, M. J., Naranjo, D., Thomas, L., Alewood, P. F., Lewis, R. J., and Craik, D. J. (1997) Solution structure and proposed binding mechanism of a novel potassium channel toxin κ-conotoxin PVIIA. *Structure 5*, 1585−1597.
(36) Savarin, P., Guenneugues, M., Gilquin, B., Lamthanh, H., Gasparini, S., Zinn-Justin, S., and Mnez, A. (1998) Three-dimensional structure of κ-conotoxin PVIIA, a novel potassium channel-blocking toxin from cone snails. *Biochemistry 37*, 5407−5416.
(37) Jacobsen, R. B., Koch, E. D., Lange-Malecki, B., Stocker, M., Verhey, J., Van Wagoner, R. M., Vyazovkina, A., Olivera, B. M., and Terlau, H. (2000) Single amino acid substitutions in κ-conotoxin PVIIA disrupt interaction with the Shaker K^+ channel. *J. Biol. Chem. 275*, 24639−24644.
(38) Garcia, E., Scanlon, M., and Naranjo, D. (1999) A marine snail neurotoxin shares with scorpion toxins a convergent mechanism of blockade on the pore of voltage-gated K channels. *J. Gen. Physiol. 114*, 141−157.
(39) Terlau, H., Boccaccio, A., Olivera, B. M., and Conti, F. (1999) The block of Shaker K^+ channels by κ-conotoxin PVIIA is state dependent. *J. Gen. Physiol. 114*, 125−140.
(40) Boccaccio, A., Conti, F., Olivera, B. M., and Terlau, H. (2004) Binding of κ-conotoxin PVIIA to Shaker K^+ channels reveals different K^+ and Rb^+ occupancies with the ion channel pore. *J. Gen. Physiol. 124*, 71−81.
(41) Olivia, C., Gonzalez, V., and Naranjo, D. (2005) Slow inactivation in voltage gated potassium channels is insensitive to the binding of pore occluding peptide toxins. *Biophys. J. 89*, 1009−1019.
(42) Jouirou, B., Mouhat, S., Andreotti, N., De Waard, M., and Sabatier, J. M. (2004) Toxin determinants required for interaction with voltage-gated K^+ channels. *Toxicon 43*, 909−914.
(43) Rodriguez de la Vega, R. C., and Possani, L. D. (2004) Current views on scorpion toxins specific for K^+-channels. *Toxicon 43*, 865−875.
(44) Huang, X., Dong, F., and Zhou, H. X. (2005) Electrostatic recognition and induced fit in the κ-PVIIA toxin binding to Shaker potassium channel. *J. Am. Chem. Soc. 127*, 6836−6849.
(45) Long, S. B., Tao, X., Campbell, E. B., and MacKinnon, R. (2007) Atomic structure of a voltage-dependent K^+ channel in a lipid membrane-like environment. *Nature 450*, 376−382.
(46) Humphrey, W., Dalke, A., and Schulten, K. (1996) VMD: Visual Molecular Dynamics. *J. Mol. Graphics 14*, 33−38.
(47) Benkert, P., Biasini, M., and Schwede, T. (2011) Toward the estimation of the absolute quality of individual protein structure models. *Bioinformatics 27*, 343−350.
(48) Bastug, T., and Kuyucak, S. (2009) Importance of the peptide backbone description in modeling the selectivity filter in potassium channels. *Biophys. J. 96*, 4006−4012.
(49) Bastug, T., and Kuyucak, S. (2011) Comparative study of the energetics of ion permeation in Kv1.2 and KcsA potassium channels. *Biophys. J. 100*, 629−636.
(50) Dominguez, C., Boelens, R., and Bonvin, A. M. (2003) HADDOCK: A protein-protein docking approach based on biochemical or biophysical information. *J. Am. Chem. Soc. 125*, 1731−1737.
(51) de Vries, S. J., van Dijk, A. D., Krzeminski, M., van Dijk, M., Thureau, A., Hsu, V., Wassenaar, T., and Bonvin, A. M. (2007) HADDOCK versus HADDOCK: New features and performance of HADDOCK2.0 on the CAPRI targets. *Proteins 69*, 726−733.
(52) Chen, P. C., and Kuyucak, S. (2012) Developing a comparative docking protocol for the prediction of peptide selectivity profiles: Investigation of potassium channel toxins. *Toxins 4*, 110−138.
(53) Phillips, J. C., Braun, R., Wang, W., Gumbart, J., Tajkhorshid, E., Villa, E., Chipot, C., Skeel, R. D., Kale, L., and Schulten, K. (2005) Scalable molecular dynamics with NAMD. *J. Comput. Chem. 26*, 1781−1802.
(54) MacKerell, A. D., Jr., Bashford, D., Bellott, M., Dunbrack, R. L., Evanseck, J. D., Field, M. J., Fischer, S., Gao, J., Guo, H., Ha, S., Joseph-McCarthy, D., Kuchnir, L., Kuczera, K., Lau, F. T. K., Mattos, C., Michnick, S., Ngo, T., Nguyen, D. T., Prodhom, B., Reiher, W. E., Roux, B., Schlenkrich, M., Smith, J. C., Stote, R., Straub, J., Watanabe, M., Wiorkiewicz-Kuczera, J., Yin, D., and Karplus, M. (1998) All-atom empirical potential for molecular modeling and dynamics studies of proteins. *J. Phys. Chem. B 102*, 3586−3616.
(55) MacKerell, A. D., Feig, M., and Brooks, C. L. (2004) Extending the treatment of backbone energetics in protein force fields. *J. Comput. Chem. 25*, 1400−1415.

(56) Kumar, S., Bouzida, D., Swensen, R. H., Kollman, P. A., and Rosenberg, J. M. (1992) The weighted histogram analysis method for free-energy calculations on biomolecules. *J. Comput. Chem. 13*, 1011−1021.